7-2011

Photoexcitation and photoionization from the 2p53p[5/2]2,3 levels in neon

M. A. Baig

I. A. Bokhari

M. Rafiq

M. A. Kalyar

T. Hussian

See next page for additional authors

Photoexcitation and photoionization from the $2p^5 3p[5/2]_{2,3}$ levels in neon

M. A. Baig,* I. A. Bokhari, M. Rafiq, M. A. Kalyar,† T. Hussian, and Raheel Ali
Atomic and Molecular Physics Laboratory, Department of Physics, Quaid-i-Azam University, 45320 Islamabad, Pakistan

N. K. Piracha
Department of Physics, John Carroll University, 20700 N. Park Boulevard, University Heights, Ohio 44118, USA
(Received 28 April 2011; published 27 July 2011)

We present measurements of the excitation spectra from the $2p^5 3p\ [5/2]_{3,2}$ levels in neon using two-step laser excitation and ionization in conjunction with an optogalvanic detection in dc and rf discharge cells. The $2p^5 3p\ [5/2]_{3,2}$ intermediate levels have been approached via the collisionally populated $2p^5 3s\ [3/2]_2$ metastable level. The Rydberg series $2p^5(^2P_{3/2})nd\ [7/2]_4$ ($12 \leqslant n \leqslant 44$), $2p^5(^2P_{3/2})ns\ [3/2]_2$ ($13 \leqslant n \leqslant 35$) and the parity forbidden transitions $2p^5(^2P_{3/2})np\ [5/2]_3$ ($13 \leqslant n \leqslant 19$) have been observed from the $2p^5 3p\ [5/2]_3$ level, whereas the $2p^5(^2P_{3/2})nd\ [7/2]_3$ ($12 \leqslant n \leqslant 44$), $2p^5(^2P_{3/2})ns\ [3/2]_2$ ($13 \leqslant n \leqslant 35$), and $2p^5(^2P_{1/2})nd'\ [5/2]_3$ ($9 \leqslant n \leqslant 12$) Rydberg series have been observed from the $2p^5 3p[5/2]_2$ level in accordance with the $\Delta J = \Delta K = \pm 1$ selection rules. The photoionization cross sections from the $2p^5 3p\ [5/2]_3$ intermediate level have been measured at eight ionizing laser wavelengths (399, 395, 390, 385, 380, 370, 364, and 355 nm) and that from the $2p^5 3p\ [5/2]_2$ level at 401.8 nm. These measurements are in excellent agreement with the experimental values reported in the literature, while the experimental data lie much below the theoretically calculated photoionization cross sections curve.

DOI: 10.1103/PhysRevA.84.013421 PACS number(s): 32.80.Fb, 32.70.Cs, 32.70.Fw, 32.80.Rm

I. INTRODUCTION

The ground state of neon is $2p^6$. The $2p^5 3s$ configuration reveals four levels, namely, $2p^5 3s\ [3/2]_{2,1}$ and $2p^5 3s'\ [1/2]_{0,1}$. The $2p^5 3s\ [3/2]_2$ and $2p^5 3s'\ [1/2]_0$ are the metastable states having lifetimes of the order of a few seconds. The $2p^5 3p$ configuration spreads over ten energy levels. The six levels, namely, $2p^5 3p\ [5/2]_{3,2}$, $[3/2]_{1,2}$, $[1/2]_{0,1}$, are associated with $2p^5(^2P_{3/2})$, whereas four levels $[3/2]_{1,2}$ and $[1/2]_{1,0}$ are associated with the $2p^5(^2P_{1/2})$ parent ion level. The excited states are designated in the $j_c K$-coupling scheme [1]. In this coupling scheme, the orbital angular momentum ℓ_2 of the excited electron couples with the total angular momentum $j_c = 3/2, 1/2$ of the core electrons to give the resultant angular momentum K as $(j_c \pm \ell_2)$. The angular momentum K is then weakly coupled with the spin angular momentum s_2 of the excited electron to yield the total angular momentum J as $(K \pm s_2)$. The energy levels are denoted as $n\ell\ [K]_J$, whereas the levels marked with a prime are associated with the $3p^5(^2P_{1/2})$ parent ion configuration. The neon emission in the visible region consists of transitions between the levels associated with the $2p^5 3p$ and $2p^5 3s$ configurations that are frequently used as reference wavelengths for data calibration. The lowest-lying levels with $J = 3$ and 2 of the $2p^5 3p$ configuration are $2p^5 3p\ [5/2]_3$ ($^3D_3$ in LS designation) at 149 657.042 1 cm^{-1} and $2p^5 3p\ [5/2]_2$ ($^3D_2$) at 149 824.2215 cm^{-1}, respectively [2]. During the past two decades, much attention has been paid to measuring the near-threshold photoionization cross section from the $2p^5 3p\ [5/2]_3$ level. Ganz *et al.* [3], using the two-step laser excitation-ionization technique in conjunction with a collimated atomic beam of the metastable neon atoms, measured the absolute value of the cross section near the threshold; the cross section remained nearly constant down to 409 nm. Subsequently, Siegel *et al.* [4] reported the cross section at a 351.1 nm ionizing laser wavelength. Recently, Claessens *et al.* [5], using the magneto-optical trap (MOT) technique, measured the photoionization cross section for this level at two laser wavelengths: 363.8 and 351.1 nm. More recently, Petrov *et al.* [6] reported the theoretical calculations for the photoionization of the $2p^5 3p[5/2]_3$ level covering the photoelectron energy range 0–2.5 eV (1 eV = 8065.54 cm^{-1}) using the configuration interaction Pauli-Fock with core polarization (CIPFCP) method. It was inferred that the cross section between the $2p^5(^2P_{3/2})$ and $2p^5(^2P_{1/2})$ ionization thresholds is strongly influenced by the $2p^5(^2P_{1/2})$ nd and ng sharp autoionizing resonances. To date, these autoionizing resonances have not been experimentally observed excited from the $2p^5 3p\ [5/2]_3$ intermediate level.

The aim of the present work was twofold: to record the photoexcitation spectrum from the $2p^5 3p\ [5/2]_3$ level and extend these measurements to locate the predicted autoionizing resonances between the $2p^5(^2P_{3/2})$ and $2p^5(^2P_{1/2})$ ionization thresholds; and secondly, to measure the absolute value of the photoionization cross sections from the $2p^5 3p\ [5/2]_3$ level at different ionizing laser wavelengths covering the photoelectron energy range up to 0.5 eV as theoretical calculations covering this region are available [6]. In the present experiments, the $2p^5 nd'\ [5/2]_3$ autoionizing resonances have not been observed when excited from the $2p^5 3p\ [5/2]_3$ level but very sharp $12d'\ [5/2]_3$ lines have been observed above the first ionization threshold when excited from the $2p^5 3p\ [5/2]_2$ level. The photoionization cross sections at eight ionizing laser wavelengths have been measured from the $2p^5 3p\ [5/2]_3$ level that are in excellent agreement with the measured literature values.

*Corresponding author:baig@qau.edu.pk or baig77@gmail.com
†Present address: Department of Physics, Sargodha University, Sargodha, Pakistan

II. EXPERIMENTAL DETAILS

The basic experimental arrangement to record the photoexcitation/photoionization spectrum and to measure the photoionization cross section is similar to that described in our earlier papers [7–10]. Briefly, it consists of a Nd:YAG laser (where YAG represents yttrium aluminum garnet) (Quantel, Brilliant-B), a TDL-90 dye laser (linewidth $\sim$0.08 cm^{-1}), a Hanna-type dye laser (linewidth $\leqslant$0.2 cm^{-1}), a neon-filled direct current (dc) discharge cell, and a radio frequency (rf) discharge cell. The $2p^5 3s\ [3/2]_2$ metastable level gets collisionally populated in a discharge. In the first step, the $2p^5 3p\ [3/2]_{3,2}$ intermediate levels were excited from the $2p^5 3s\ [3/2]_2$ level, using a dye laser charged with the Di Cyan Methylene (DCM) (Exciton, USA) and pumped by the light from the second harmonic (532 nm) of the Nd:YAG laser. The second-step dye laser was charged with the Stilbene 420 dye (Exciton, USA) and pumped by the light from the third harmonic (355 nm) of the same Nd:YAG laser. Since the lifetimes of these excited states are 19.4 and 19.6 ns, respectively [11], recording the $2p^5 nd$ Rydberg series from the intermediate levels required the second dye laser to be temporally delayed with respect to the first dye laser by about 4 ns to ensure the pure two-step excitation process. The pulse width of the Nd:YAG laser was 5 ns and it was operated at a repetition rate of 10 Hz. A computer-controlled stepper motor was used to scan the second dye laser over the desired wavelength range. A single motor step advances about 0.02 cm^{-1} on the energy scale. Both the lasers were linearly polarized and overlapped in the interaction region of the discharge cell. Beam splitters were inserted in the optical path of the second dye laser beam to divide it into three parts. One portion of the laser beam was directed through a 1-mm-diameter aperture to an argon-filled discharge cell. The second portion, about 10% of the beam, was passed through a 2-mm-thick solid etalon Free Spectral Range (FSR) 1.65 cm^{-1}) and the third portion of the beam was directed to a neon-filled hollow cathode lamp, which produced well-distributed neon lines that have been used as reference wavelengths to determine the wavelengths of the observed spectral lines. The three signals were simultaneously recorded using three boxcar averagers (SR250) and the data were stored on a computer through a General Purpose Interface Bus (GPIB) card for subsequent analysis. The term energies of the observed Rydberg levels have been determined by adding the energy of the intermediate level to the laser excitation energies. The maximum uncertainty in the extracted term energies of the Rydberg levels is $\pm$0.2 cm^{-1}.

For the measurement of the photoionization cross sections from the $2p^5 3p\ [5/2]_{3,2}$ intermediate levels near the first ionization threshold, the diameter of the exciting laser was set $\approx$2.5 mm while the cross-sectional area of the ionizing laser was calculated at each ionizing laser wavelength. Both the dye lasers were linearly polarized with their electric vectors parallel to each other. In each experiment, the intensity of the exciting laser was kept fixed, while the intensity of the ionizing laser was varied by inserting neutral density filters (Edmund Optics), and on each insertion the corresponding dye laser energy was measured. The ion signal was registered on a storage oscilloscope and on a computer for subsequent analysis.

III. RESULTS AND DISCUSSION

A. Photoexcitation spectrum from the $2p^5 3p\ [5/2]_3$ level

We have used two sources to generate the neon discharge: a dc discharge cell and a rf discharge cell to record the excitation spectrum from the $2p^5 3p\ [5/2]_3$ level. In these discharge cells, the $2p^5 3s\ [3/2]_2$ metastable level gets populated due to collisions. To record the two-step excitation spectrum from the $2p^5 3p\ [5/2]_3$ level at 149 657.042 cm^{-1}, it was populated from the $2p^5 3s\ [3/2]_2$ level by tuning the first dye laser at 640.4 nm. The second dye laser was scanned from 428 to 410 nm covering the region up to the first ionization threshold $2p^5(^2P_{3/2})$ of neon. The dipole-allowed transitions associated with the excitation from the $2p^5 3p\ [5/2]_3$ level are

$$\begin{aligned} 2p^5 3p[5/2]_3 &\rightarrow 2p^5(^2P_{3/2})ns\ [3/2]_2 \\ &\rightarrow 2p^5(^2P_{3/2})nd\ [7/2]_{3,4},\ [5/2]_{2,3},\ [3/2]_2 \\ &\rightarrow 2p^5(^2P_{1/2})nd'\ [5/2]_{2,3},\ [3/2]_2. \end{aligned}$$

In Fig. 1(a), we show the spectrum recorded using the dc discharge covering the energy region from 23 550 to 24 270 cm^{-1} showing a distinct Rydberg series. The strong lines are identified as the $2p^5 nd\ [7/2]_4$ Rydberg series ($13 \leqslant n \leqslant$ limit) and the accompanying sharp series is identified as $2p^5 ns\ [3/2]_2$ ($14 \leqslant n \leqslant$ limit). There are some very weak lines adjacent to the $2p^5 nd\ [7/2]_4$ series that have been identified as $2p^5 nd\ [5/2]_3$. The level identifications are based on the observed line intensities in comparison with the calculated line strengths of Faust and McFarlane [12] as well as their quantum defects that are equal to the lower members of the series listed by Kaufman and Minnhagen [2]. The most intense transitions are those which follow the $\Delta K = \Delta J = \Delta \ell = +1$ selection rules, whereas the other possible transitions follow $\Delta K = \Delta J = 0$. Faust and McFarlane [12] calculated the relative line strength of the $2p^5 nd\ [7/2]_4$ transitions nearly 4.5 times stronger than the $2p^5 nd\ [5/2]_3$ transitions, and indeed, our experimental results are in conformity with these calculations. The weak and broad lines, adjacent to the strong $2p^5 nd\ [7/2]_4$ series on the higher energy side, are identified as the parity forbidden transitions $2p^5 3p\ [5/2]_3 \rightarrow 2p^5 np\ [5/2]_3$ that emerged either due to collisions of the Rydberg atoms or due to the presence of an electric field in the dc hollow cathode cell, that might mix states at high n values. Adjacent to the series convergence, two sharp lines are identified as excitations from the collisionally populated $2p^5 3p\ [1/2]_1$ level to the $2p^5 7d'\ [3/2]_2$ and $2p^5 10s\ [3/2]_2$ levels, respectively. Interestingly, the intensities of the $2p^5 nd\ [7/2]_4$ series decrease in accord with the n^{-3} power showing an unperturbed nature of the Rydberg series.

In order to record this spectrum in a nearly field-free environment, we repeated this experiment using a rf discharge cell. In Fig. 1(b) we show the spectrum covering the region from 23 750 to 24 352 cm^{-1}, similar to Fig. 1(a). The dipole-allowed spectral lines are sharp, whereas the parity-forbidden transitions are absent, reflecting the nonexistence of any field effects that might have been present in the dc discharge setup. The $2p^5 nd\ [7/2]_4$ series have been extended to a much higher principal quantum number. A sharp line between $n = 15$ and 16 and two sharp lines between $n = 18$ and 19 members of the $2p^5 nd\ [7/2]_4$ series have been identified as transitions from the collisionally populated $2p^5 3p\ [1/2]_1$ level to the $2p^5 9s\ [3/2]_2$ and $2p^5 8d\ [1/2]_1$, $[3/2]_2$ levels, respectively. Adjacent to the

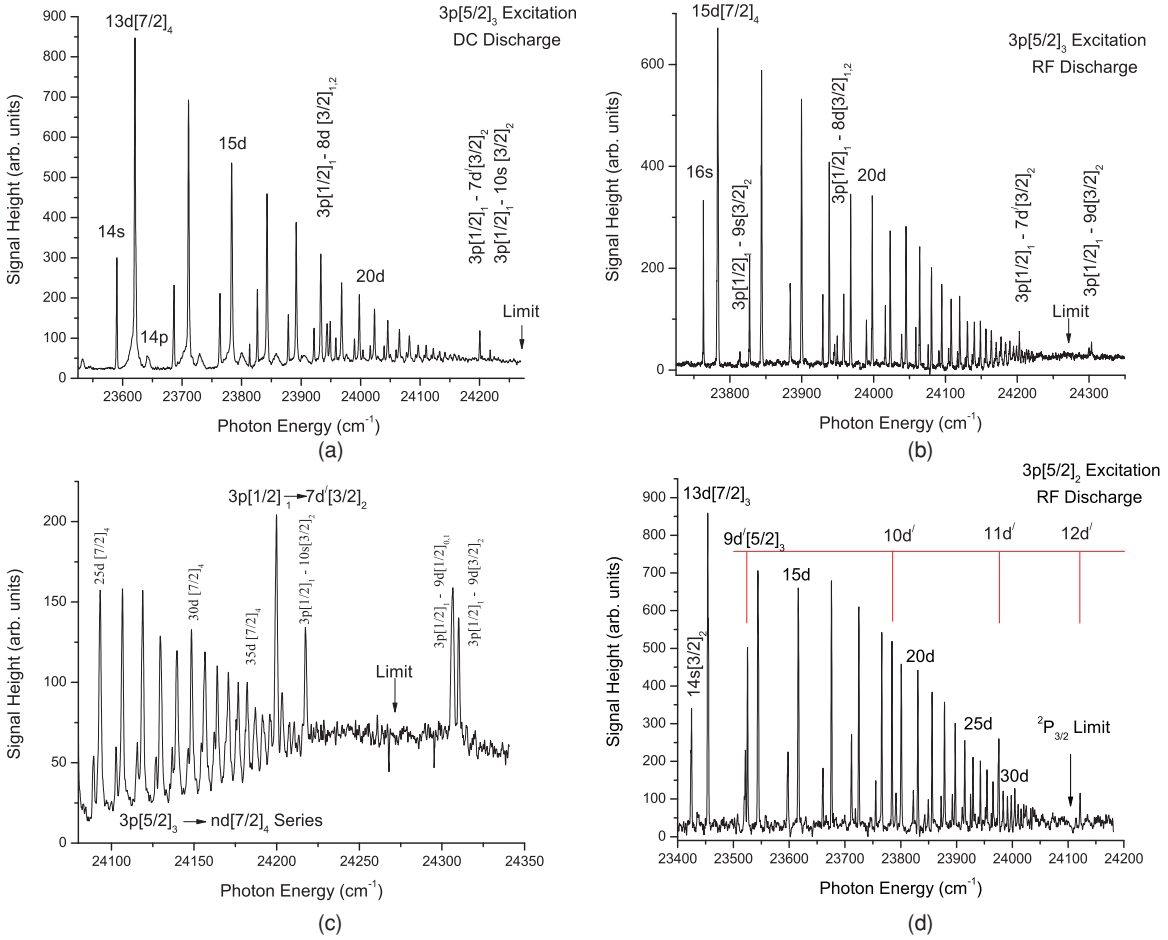

FIG. 1. (Color online) (a) The $2p^5nd$ $[7/2]_4$ ($13 \leqslant n \leqslant$ limit) and ns $[3/2]_2$ ($14 \leqslant n \leqslant$ limit) Rydberg series of neon excited from the $2p^53p$ $[5/2]_3$ intermediate level using a dc discharge cell. The lines near the limit are due to excitation from the collisionally populated $3p$ $[1/2]_1$ level. (b) The $2p^5nd$ $[7/2]_4$ ($15 \leqslant n \leqslant$ limit) and ns $[3/2]_2$ ($16 \leqslant n \leqslant$ limit) Rydberg series of neon excited from the $2p^53p$ $[5/2]_3$ intermediate level using a rf discharge cell. The lines in the vicinity of the series limit are due to excitation from the collisionally populated $3p$ $[1/2]_1$ level. (c) The $2p^5nd$ $[7/2]_4$ ($25 \leqslant n \leqslant$ limit) and ns $[3/2]_2$ ($25 \leqslant n \leqslant$ limit) Rydberg series of neon excited from the $2p^53p$ $[5/2]_3$ intermediate level showing the structure in the vicinity of the series limit. The lines due to excitation from the $3p$ $[1/2]_1$ level appear with good intensity as compared to those in (a). (d) The $2p^5nd$ $[7/2]_3$ ($13 \leqslant n \leqslant$ limit) and ns $[3/2]_2$ ($14 \leqslant n \leqslant$ limit) Rydberg series of neon excited from the $2p^53p$ $[5/2]_2$ intermediate level using a rf discharge cell. The lines associated with the $2p^5(^2P_{1/2})$ limit appear much stronger here, whereas these were absent in the excitation from the $2p^53p$ $[5/2]_3$ intermediate level. The $12d'$ $[5/2]_3$ line lies above the first ionization limit but its width is comparable to the lines lying below the ionization limit.

series limit (24 272.708 cm^{-1}), two lines have been observed and identified as $2p^53p$ $[1/2]_1 \rightarrow 2p^57d'$ $[3/2]_2$ and $2p^510s$ $[3/2]_2$ transitions, respectively. An additional line identified as $2p^53p$ $[1/2]_1 \rightarrow 2p^59d$ $[3/2]_2$ is observed just above the first ionization threshold.

The lines associated with excitation from the $2p^53p$ $[1/2]_1$ level are very weak as compared to those from the $2p^53p$ $[5/2]_3$ level, which reveals the relative populations of these two low-lying levels. The optogalvanic signal remains nearly constant in the region from 24 200 to 24 300 cm^{-1}, whereas the signal intensities near the ionization threshold are very low, apparently due to the low efficiency of the dye laser (stilbene-420) in this region. The spectrum close to the ionization threshold was recorded using a more efficient dye (stilbene-411, Exciton, USA) for this region. Figure 1(c) shows the resulting spectrum covering the laser energy region from 24 050 to 24 350 cm^{-1} revealing the well-developed Rydberg series close to the ionization threshold that has been extended up to $n = 42$. The additional lines $2p^57d'$ $[3/2]_2$, $2p^510s$ $[3/2]_2$, $2p^59d$ $[1/2]_{0,1}$, and $[3/2]_2$ excited from the $3p[1/2]_1$ level are very prominent in this spectrum. The location of the first ionization threshold is marked with an arrow, and evidently the optogalvanic signal around the ionization threshold remains invariable. We have not observed any line associated with the $2p^5(^2P_{1/2})$ limit in this region although the $2p^5nd'$ $[5/2]_3$ autoionizing resonances were anticipated above the ionization threshold. The $2p^511d'$ $[5/2]_3$ line should have appeared around 24 142.96 cm^{-1}, lying below the limit, and the $2p^512d'$ $[5/2]_3$ line at 24 288.06 cm^{-1} just above the ionization threshold. The absence of these lines clearly ascribes the nonexistence of the autoionizing resonances associated with excitation from the $2p^53p$ $[5/2]_3$ lower level, although Petrov *et al.* [6] have theoretically predicted the location and line shape of the $2p^512d'$ $[5/2]_3$ line. In our earlier experiments [13], using $2p^53p'$ $[3/2]_2$

as an intermediate level, we have observed the $2p^5 11d'$ $[5/2]_3$ autoionizing resonance, very sharp and strong with a nearly symmetric line shape. The present experimental results supplement the idea of very low transition probabilities for excitations from the $2p^5(^2P_{3/2})$-based levels to the $2p^5(^2P_{1/2})$-based levels. Interestingly, we have not observed any transition from the $2p^5 3p$ $[5/2]_2$ level that lies only 167.18 cm^{-1} above the $2p^5 3p$ $[5/2]_3$ level, whereas a number of transitions have been observed from the $2p^5 3p$ $[1/2]_1$ level that lies about 1400 cm^{-1} below the $2p^5 3p$ $[5/2]_3$ level. In the next section, we present the excitation spectrum from the $2p^5 3p$ $[5/2]_2$ level covering the region around the first ionization threshold.

B. Photoexcitation spectrum from the $2p^5 3p[5/2]_2$ level

The $2p^5 3p$ $[5/2]_2$ level lies at 149 824.2215 cm^{-1} [2], about 167.18 cm^{-1} above the $2p^5 3p[5/2]_3$ level. In order to record the excitation spectrum form this level, it was populated by tuning the first dye laser at 633.6 nm and the second dye laser was scanned from 430 to 410 nm. The dipole-allowed transitions associated with this excitation scheme are

$$\begin{aligned} 2p^5 3p[5/2]_2 &\rightarrow 2p^5(^2P_{3/2})ns\ [3/2]_{1,2} \\ &\rightarrow 2p^5(^2P_{3/2})nd\ [7/2]_3,\ [5/2]_{3,2},\ [3/2]_2 \\ &\rightarrow 2p^5(^2P_{1/2})nd'\ [5/2]_{3,2},\ [3/2]_{1,2} \\ &\rightarrow 2p^5(^2P_{1/2})ns'\ [1/2]_1. \end{aligned}$$

The spectrum is presented in Fig. 1(d) showing two well-resolved Rydberg series. The strong series is assigned as $2p^5 nd$ $[7/2]_3$ and the weak series as $2p^5 ns$ $[3/2]_{1,2}$ in accordance with the selection rules (see above). The unambiguous assignments have been made using the theoretically calculated relative line strengths of the dipole-allowed transitions. Faust and McFarlane [12] reported the relative line strengths for the $2p^5 3p$ $[5/2]_2 \rightarrow 2p^5 nd$ $[7/2]_3$ transitions nearly 4.7 times stronger than the $2p^5 3p$ $[5/2]_2 \rightarrow 2p^5 nd$ $[5/2]_2$ transitions. The later series are too weak to be detected in the present experiments. The observed Rydberg series are assigned as $2p^5 nd$ $[7/2]_3$ $(12 \leqslant n \leqslant 44)$, $2p^5 ns$ $[3/2]_2$ $(12 \leqslant n \leqslant 35)$, and $2p^5 ns$ $[3/2]_1$ $(13 \leqslant n \leqslant 17)$. In addition, we have observed the $2p^5 nd'$ $[5/2]_3$ $(9 \leqslant n \leqslant 12)$ series associated with the $2p^5(^2P_{1/2})$ limit. The $2p^5 12d'$ $[5/2]_3$ line lies just above the first ionization threshold, marked by an arrow in the figure. It was expected that the width of this line would be larger than that of the lines lying below the first ionization threshold due to its interaction with the continuum. However, it is observed that the widths of the $2p^5 11d'$ $[5/2]_3$ and $2p^5 12d'$ $[5/2]_3$ lines are almost similar, reflecting negligible interaction between the $2p^5(^2P_{3/2})\,\varepsilon\ell$ continuum channels and the $2p^5(^2P_{1/2})12d'$ $[5/2]_3$ discrete level.

We have determined the term energies of all the levels by adding the energies of the intermediate levels to the laser excitation energies that are found to be in excellent agreement with the earlier reported values. The quantum defects μ_ℓ associated with each energy level have been calculated using the Rydberg relation:

$$E_n = V_{\text{ion}} - \frac{R_y}{(n-\mu_\ell)^2}. \tag{1}$$

Here E_n (cm^{-1}) is the term energy of the level, R_y is the mass-corrected Rydberg constant for neon 109 734.332 cm^{-1}, and V_{ion} is the ionization potential of neon 173 929.75 $\pm$ 0.06 cm^{-1} [2]. The Rydberg series can be extended up to much higher principal quantum numbers by improving the laser linewidth and signal-to-noise ratio. However, the main objective of the present work was to locate the autoionizing resonances rather than to extend the series to higher n values and to measure the photoionization cross sections from the excited levels in neon. Knowing the absolute value of the photoionization cross section at the ionization threshold, the oscillator strengths of the Rydberg series can be calculated. Gallagher [14] inferred that the oscillator strength of an unperturbed Rydberg series decreases as n^{-3}. Any deviation of the scaling from $1/n^3$ is attributed to some hidden perturbations. Evidently, the line intensities of the observed series show the $1/n^3$ behavior (see Figs. 1 and 2). In the following section we present the measurements of the photoionization cross section from the $2p^5 3p$ $[5/2]_{3,2}$ levels at different ionizing laser wavelengths.

C. Measurements of photoionization cross section

Photoionization cross section is a measure of the probability of how much ionization is produced by the photons interacting with the sample under study. The measured values of the photoionization cross section of atoms have a number of applications in space, astrophysics, radiation protection, and laser designing. The knowledge of photoionization cross sections is not only important from the ground states of atoms but also from the excited states. Furthermore, the concept of cross section is important in understanding the interaction of radiation with matter, which is a basic phenomenon in nature. There are a number of methods for the measurement of photoionization cross sections. Babin and Gange [15] used a hollow cathode lamp to measure the photoionization cross section of the refractory elements. Stockhausen *et al.* [16] used a hollow cathode lamp to measure the photoionization cross section of the auto-ionizing lines of copper. In our earlier studies [17], the photoionization cross sections from the $2p^5 3p'$ $[1/2]_1$ level at the $2p^5\ ^2P_{1/2}$ ionization threshold was reported as 4.7 ± 0.6 Mb (1 Mb $= 10^{18}$ cm^2), from the $2p^5 3p'$ $[3/2]_2$ level at 419.3 nm ionizing laser wavelength as 4.8 ± 1.0 Mb, and from the $2p^5 3p$ $[5/2]_3$ level at 399.1 nm ionizing laser wavelength as 5.7 ± 1.5 Mb. The prime motivation behind the present work was to measure the absolute value of the photoionization cross section from the $2p^5 3p$ $[5/2]_3$ level at the first ionization threshold, at a corresponding ionizing laser wavelength 411.99 nm. As explained above, the near-threshold region contains a few spectral lines, excited from the $2p^5 3p$ $[1/2]_1$ level, that hampers our attempt to determine the cross section at the first ionization threshold.

We have measured the photoionization cross section from the $2p^5 3p$ $[5/2]_{3,2}$ intermediate levels at eight ionizing laser wavelengths; from 399 to 355 nm with 5 nm incremental steps, using the two-step ionization and saturation technique as described by Burkhardt *et al.* [18], He *et al.* [19], Saleem *et al.* [20], and Haq *et al.* [21]. The experiments have been performed with assumptions that the intensity of the ionizing laser was larger than that required for saturating the intermediate level,

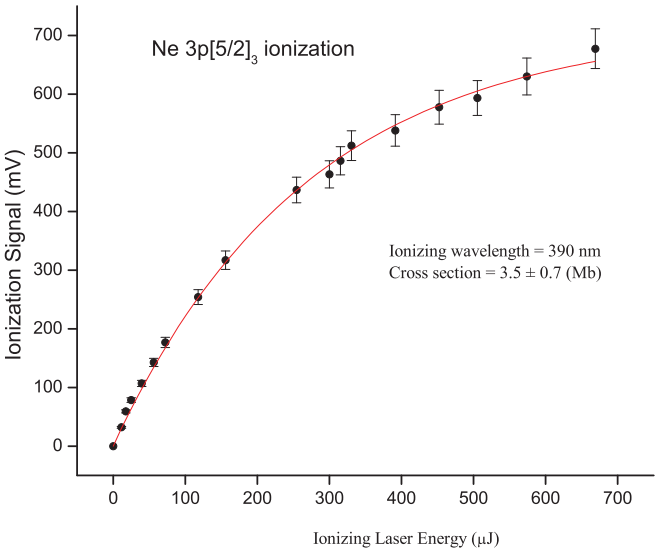

FIG. 2. (Color online) The saturation curve used to determine the absolute value of the cross section σ (Mb) from the $3p[5/2]_3$ intermediate level at 390 nm ionizing laser wavelength. The solid line represents the least-square fit of Eq. (2). The errors on the data point result from pulse-to-pulse fluctuations in the signal.

and that the spontaneous emission was ignored during the 5 ns laser pulse. It was further assumed that the transitions remain saturated during the laser pulse, and the intensity of the ionizing laser beam was uniformly distributed and linearly polarized. Under these assumptions an empirical relation was developed to determine the cross section at the ionizing laser wavelength:

$$Z = \frac{Q}{\mathrm{eV_{vol}}} = N_0 \left[1 - \exp\left(-\frac{\sigma U}{2\hbar\omega A}\right)\right], \tag{2}$$

where Z is the total number of ions collected per unit volume, e (C) is the electronic charge, N_0 (cm^{-3}) is the density of excited atoms, A (cm^2) is the cross-sectional area of the ionizing laser beam, U (J) is the total energy per ionizing laser pulse, $h\omega$ (J) is the energy per photon of the ionizing laser beam, V_{vol} (cm^3) is the laser interaction volume, and σ (cm^2) is the cross section for photoionization. In this technique, the first laser produces a column of excited vapors and the second laser, tuned to a fixed wavelength, photoionizes the atoms from the excited state. As the intensity of the second laser is increased, the number of ions increases as well, and a saturation is attained if all the excited atoms are ionized. A complete saturation can only be achieved with a top-hat-shaped laser pulse, whereas the wings in the Gaussian-shaped laser pulse hinder the complete saturation. Since the laser beams in the present work are Gaussian, their spatial profiles were monitored by scanning a *p-i-n* photodiode across their diameters and their spot sizes were established using the distance at which their intensities fall to $1/e^2$. The first dye laser at 640.4 nm excites the atoms from the $2p^5 3s\ [3/2]_2$ metastable state to the $2p^5 3p\ [5/2]_3$ intermediate level and the second dye laser promotes the atoms from the intermediate level to the ionization continuum. The required ionizing wavelengths were achieved by frequency mixing the output from the dye laser (TDL-90) and the fundamental laser (1064 nm) from the Nd:YAG laser, whereas the ionizing wavelength 355 nm was obtained from the third harmonic of the Nd:YAG laser. The first dye laser beam spot diameter was ≈2.5 mm and its energy density was adjusted such that the signal for the $2p^5 3s\ [3/2]_2 \rightarrow 2p^5 3p\ [5/2]_3$ transition remains saturated. The second dye laser beam, which was delayed by about 4 ns, was also passed through the discharge cell through an ≈2 mm aperture. The spot size of the exciter laser was larger than the spot size of the ionizing laser that eliminates the problems associated with the spatial overlapping of the exciter and the ionizer laser pulses. The area of the overlap region in the confocal limit is calculated by using the relation described in [22]:

$$A = \pi\omega_o^2 \left[1 + \left(\frac{Z}{Z_0}\right)^2\right]. \tag{3}$$

Here $\omega_o = \lambda/\pi\theta$ is the beam waist, θ is the beam divergence ($\leqslant$1 m rad.), Z is the aperture distance from the interaction region, and $Z_0 = \pi\omega_o^2/\lambda$. The intensity of the first laser is kept constant, while the intensity of the second laser is varied by inserting different neutral density filters.

The ion signal is registered on the oscilloscope as a function of the ionizing laser energy for further processing. A typical data for the photoionization signal from the $2p^5 3p\ [5/2]_3$ level as a function of variation of the ionizing laser energy from 0 to 750 μJ at 390 nm is shown in Fig. 2. The solid line, which passes through the data points, is a least-square fit to Eq. (2). The fitting of the experimental data yields the value of the photoionization cross section as 3.5 ± 0.6 Mb. It is evident from the figure that as the laser energy increases the ion signal increases rapidly and then changes slowly. The multistep photoionization process greatly depends on the flux of the ionizing laser pulse, and a complete saturation curve yields a more accurate value of the photoionization cross section. Unfortunately, we have not been able to achieve the complete saturations for the photoionization from the $2p^5 3p\ [5/2]_3$ intermediate level in the present work, a limitation of our experimental system. In a similar way, we have determined the absolute values of the photoionization cross sections at different ionizing laser wavelengths: 399, 395, 390, 385, 380, 370, 364, and 355 nm. The corresponding values of the photoionization cross sections at these wavelengths have been determined as 5.7 ± 1.0, 4.2 ± 0.8, 3.5 ± 0.6, 3.0 ± 0.6, 2.7 ± 0.5, 2.3 ± 0.4, 2.2 ± 0.4, and 2.0 ± 0.4 Mb, respectively. In addition, using the same technique, we have measured the absolute value of the photoionization cross section from the $2p^5 3p\ [5/2]_2$ level at 410.8 nm ionizing laser wavelength as 3.8 ± 0.7 Mb. It is worth mentioning that the main sources of uncertainty in the measurement of the absolute value of the photoionization cross section are the uncertainty in the laser energy measurement and the cross-sectional area of the ionizer laser beam in the interaction region. The uncertainties in the energy measurements are due to the energy meter (±5%) and the pulse-to-pulse variations in the laser energy (±5%). The uncertainty in the area measurement of the spatial beam profile of the ionizer laser (±15%) is due to the spontaneous decay during the laser pulse (±10%). The overall uncertainty in the measured cross sections does not exceed 20%. Samson *et al.* [23,24] reported the photoionization cross section of neon at the $2p^5\ ^2P_{1/2}$ ionization threshold as 6.38 Mb. Lee

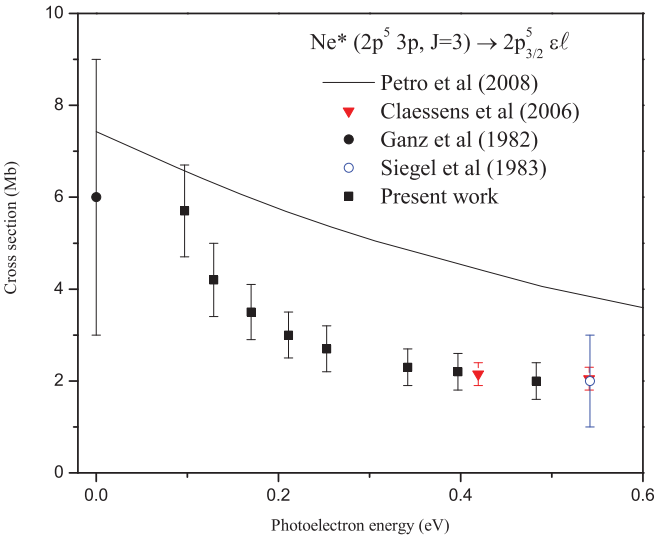

FIG. 3. (Color online) Photoionization cross sections from the $2p^5 3p\ [5/2]_3$ level at different ionizing laser wavelengths corresponding to photoelectron energy range 0–0.6 eV. The solid line is the PF. CIPE calculations are shown for Petrov *et al*. [6] as well as the experimental data for Ganz *et al*. [3], Siegel *et al*. [4], Claessens *et al*. [5], and the present work.

and Weissler [25] determined the cross section as 5.8 Mb. James *et al*. [26] gave the ratio of the cross section as 2.18 of $^2P_{3/2}$ at the ground state and to the number of ions produced in $^2P_{1/2}$ at the excited state. Ganz *et al*. [3] reported the photoionization cross section from the $2p^5 3p\ [5/2]_3$ level at the first ionization threshold as 6 ± 3 Mb, Siegel *et al*. [4] reported this cross section as 2 ± 1 Mb at 351.1 nm, and Claessens *et al*. [5] measured its value as 2.15 ± 0.25 and 2.05 ± 0.25 Mb at 363.8 and 351.1 nm, respectively. Recently, Petrov *et al*. [6] calculated the cross section at the first ionization threshold as 7.28 Mb. In Fig. 3, we reproduce the existing data on the photoionization cross section along with our data covering the excess energy up to 0.6 eV. The solid line is the theoretical calculations by Petrov *et al*. [6]. The data obtained in the present studies are in excellent agreement with the previously measured values, while the data lie lower than the theoretically calculated photoionization curve. In Table I we have tabulated the previously measured values of the photoionization cross sections from the $2p^5 3p\ [5/2]_{3,2}$ intermediate levels at different ionizing laser wavelengths along with the present data.

IV. CONCLUSION

Using the two-step excitation and ionization technique, we have recorded the photoexcitation spectra from the $2p^5 3p\ [5/2]_3$ level revealing the Rydberg series: $2p^5(^2P_{3/2})nd\ [7/2]_4$ $(12 \leqslant n \leqslant 44)$, $2p^5(^2P_{3/2})ns\ [3/2]_2$ $(13 \leqslant n \leqslant 35)$, and parity forbidden transitions $2p^5 np\ [5/2]_3$ for $(13 \leqslant n \leqslant 19)$. From the $2p^5 3p\ [5/2]_2$ level, the observed Rydberg series are $2p^5(^2P_{3/2})nd\ [7/2]_3$ $(12 \leqslant n \leqslant 44)$, $2p^5(^2P_{3/2})ns\ [3/2]_2$ $(13 \leqslant n \leqslant 35)$, and $2p^5(^2P_{1/2})nd'\ [5/2]_3$ $(9 \leqslant n \leqslant 12)$. The dominating series are those in which ΔJ and ΔK change in the same direction, i.e., $\Delta J = \Delta K = +1$. The photoionization cross sections from the $2p^5 3p\ [5/2]_{3,2}$ intermediate levels have been measured at eight ionizing laser wavelengths near the first ionization threshold using the saturation technique. Our measured cross sections are in excellent agreement with the experimentally known values but deviate from the theoretical curve. It will be interesting to repeat these measurements using the MOT technique.

ACKNOWLEDGMENTS

We are grateful to the Higher Education Commission, Quaid-i-Azam University, and the Pakistan Science

TABLE I. Photoionization cross sections from the $2p^5 3p[5/2]_3$ and $2p53p[5/2]2$ levels of neon.

Present work			Previous work			
Ionizing laser wavelength (nm)	Excess energy (eV)	Photoionization cross section (Mb)	Ionizing laser wavelength (nm)	Excess energy (eV)	Photoionization cross section (Mb)	References
(a) $2p^5 3p[5/2]_3$						
			411.99	0	6 ± 3	[3]
			411.99	0	7.28	[6]
399	0.098	5.7 ± 1.0	399.1	0.097	7.15 ± 1.0	[17]
395	0.129	4.2 ± 0.8				
390	0.170	3.5 ± 0.6				
385	0.211	3.0 ± 0.6				
380	0.253	2.7 ± 0.5				
370	0.341	2.3 ± 0.4				
364	0.397	2.2 ± 0.4	363.8	0.4	2.15 ± 0.25	[5]
355	0.483	2.0 ± 0.4				
			351.1	0.521	2.15 ± 0.25	[5]
			351.1	0.521	2 ± 1	[4]
(b) $2p53p[5/2]2$						
Ionizing laser wavelength (nm)			Excess energy (eV)		Cross section (Mb)	
401.8			0.097		3.8 ± 0.7	

Foundation under project PSF(134) for the financial assistance to conduct the experimental work. M.A.B. is thankful to Professor Hotop, Kaiserslautern University, Germany for many illuminating discussions on this subject.

[1] R. D. Cowan, *The Theory of Atomic Structure and Spectra* (University of California, Berkeley, 1981).
[2] V. Kaufman and L. Minnhagen, J. Opt Soc. Am. **62**, 92 (1972).
[3] J. Ganz, B. Lewandowski, A. Siegel, W. Bussert, H. Waibel, M.-W. Ruf, and H. Hotop, J. Phys B **15**, L485 (1982).
[4] A. Siegel, J. Ganz, W. Bussert, and H. Hotop, J. Phys B **16**, 2945 (1983).
[5] B. J. Claessens, J. P. Ashmore, R. T. Sang, R. W. MacGillivray, H. C. W. Beijerinck, and E. J. D. Vredenbregt, Phys. Rev. A **73**, 012706 (2006).
[6] I. D. Petrov, V. L Sukhorukov, and H. Hotop, J. Phys B **41**, 065205 (2008).
[7] S. Hussain, M. Saleem, M. Rafiq, and M. A. Baig, Phys. Rev. A **74**, 022715 (2006).
[8] S. Mahmood, N. Amin, S. U. Haq, N. M. Shaikh, S. Hussain, and M. A. Baig, J. Phys B **39**, 2299 (2006).
[9] S. Hussain, M. Saleem, and M. A. Baig, Phys. Rev. A **76**, 012701 (2007).
[10] M. A. Baig, S. Mahmood, R. Mumtaz, R. Rafiq, M. A. Kalyar, S. Hussain, and R. Ali, Phys. Rev. A **78**, 032524 (2008).
[11] A. A. Radzig and B. M. Smirnov, *Reference Data on Atoms, Molecules, and Ions* (Springer-Verlag, Berlin, 1985).
[12] W. L. Faust and R. A. McFarlane, J. Appl. Phys. **35**, 2010 (1964).
[13] M. Aslam, Ph.D. thesis, Quaid-i-Azam University, Islamabad, Pakistan, 2000 (unpublished).
[14] T. F. Gallagher, *Rydberg Atoms* (Cambridge University, Cambridge, England, 1994).
[15] F. Babin and J. M. Gange, Appl. Phys. B **54**, 35 (1992).
[16] G. Stockhausen, W. Mende, and M. Kock, J. Phys B **29**, 665 (1996).
[17] S. Mahmood, N. M. Shaikh, M. A. Kalyar, M. Rafiq, N. K. Piracha, and M. A. Baig, J. Quant. Spectrosc. Radiat. Transf. **110**, 1840 (2009).
[18] C. E. Bukhardt, J. L. Libbert, Xu Jian, J. J. Leventhal, and J. D. Kelly, Phys Rev. A **38**, 5949 (1988).
[19] L. W. He, C. E. Bukhardt, M. Ciocca, and J. J. Leventhal, Phys. Rev. A **51**, 2085 (1995).
[20] M. Saleem, S. Hussain, M. Rafiq, and M. A. Baig, J. Phys B **39**, 5025 (2006).
[21] S. U. Haq, M. A. Kalayar, M. Rafiq, R. Ali, N. K. Piracha, and M. A. Baig, Phys. Rev. A **79**, 042502 (2009).
[22] W. Demtroeder, *Laser Spectroscopy Basic Concepts and Instruments* (Springer-Verlag, Berlin, 1998).
[23] J. A. R. Samson, L. Lin, G. N. Hadded, and G. C. Angel, J. Phys. IV C1 **1**, 99 (1991).
[24] J. A. R. Samson and W. C. Stolte, J. Electron Spectrosc. Relat. Phenom. **123**, 265 (2002).
[25] B. P. Lee and G. L. Weissler, Proc. R. Soc. London, Ser. A **220**, 71 (1953).
[26] J. A. R. Samson and R. B. Cairns, Phys. Rev. **173**, 80 (1968).